International Journal of Peptide Research and Therapeutics (2021) 27:2931–2943
https://doi.org/10.1007/s10989-021-10301-0

A Re-evaluation of the Free Energy Profiles for Cell-Penetrating Peptides Across DOPC Membranes

B. T. Kumara[1] · N. K. Wijesiri[2] · P. V. G. M. Rathnayake[1] · R. J. K. U. Ranatunga[1,2]

Accepted: 10 October 2021 / Published online: 25 October 2021

Abstract
Cell penetrating peptides (CPPs) hold immense potential for the transport of therapeutic agents to their active targets, due to their low cytotoxicity and high transduction efficiency. Adoption of CPPs as delivery systems, and development of novel peptides has been hampered by the variety of mechanisms and complexity of factors involved in cellular uptake. Quantitatively analyzing these systems is further hindered by the inability to compare data among reports due to varying experimental conditions. In this study we investigate the translocation of seventeen CPPs, representing cationic, amphipathic and hydrophobic physicochemical classes, through a DOPC membrane using molecular dynamics simulations. Free energy profiles for individual peptides inserting into the lipid bilayer were generated giving insight into both the approach and adsorption of different CPPs to cell membranes, and the feasibility of their direct translocation. The control of physical conditions and composition allows objective comparison of different peptides and analyze the effect of sequence on the adsorption and translocation energetics. Our results indicate that positively charged residues impart repulsion, while hydrophobic residues increase bilayer interaction. This study is the first step in fully understanding the processes and energetics involved in the passive translocation mechanisms of CPPs, which usually involve multiple peptides.

Keywords Cell penetrating peptides · Molecular dynamics · Free energy

Introduction

Translocation through the plasma membrane has become a major limiting step for the cellular delivery of macromolecular therapeutics. Cell membranes are effectively impermeable to many hydrophilic compounds, unless their permeation is facilitated by a dedicated transport system (Jobin et al. 2019; Said Hassane et al. 2010). Many hydrophilic compounds, including promising therapeutic agents, fail to reach their intracellular targets because they cannot spontaneously cross biological membranes (Ragin et al. 2002; Sagan 2013; Gräslund et al. 2011; Trabulo et al. 2010). As a consequence, much interest exists in developing alternate ways to facilitate this translocation.

During the last 20 years, short peptides with the ability to permeate mammalian cell membranes have been investigated widely (Sagan 2013). They have been referred to by different names such as Trojan peptides, protein transduction domains, membrane translocating sequences or most commonly as Cell penetrating peptides (CPPs). CPPs are diverse; but generally contain 5–30 amino acid residues (Gräslund et al. 2011; Ma et al. 2015). They are water soluble and can be classified into three main classes based on the physico-chemical natures of the sequences, namely, cationic, amphipathic and hydrophobic. CPPs possess the capacity to ubiquitously cross cellular membranes without causing significant membrane damage (Agrawal et al. 2016). More importantly these peptides are capable of internalizing biologically active cargoes bound to them (Schmidt et al. 2010; Lundberg and Langel 2003).

The uptake mechanisms of CPPs depend on various factors such as the physical and chemical nature, and concentration of CPPs, and the properties of the membrane (Gräslund et al. 2011). There are thought to be two major uptake mechanisms, i.e., the endocytotic (energy dependent) pathways and the direct (energy-independent) translocation

✉ R. J. K. U. Ranatunga
udayana.ranatunga@sci.pdn.ac.lk

[1] Postgraduate Institute of Science, University of Peradeniya, Peradeniya, Sri Lanka

[2] Department of Chemistry, University of Peradeniya, Peradeniya, Sri Lanka

(Choe 2020; Yesylevskyy et al. 2009). Experimental evidence exists to show that there is direct translocation of CPPs across the membrane, which does not rely on binding receptors. There are various models to explain the direct translocation such as the carpet-like model, pore formation, inverted micelle formation, and the membrane thinning model (Silva et al. 2019). The internalization mechanism of CPPs can be attributed to endocytosis under certain conditions. Molecular simulations have confirmed the strong attraction between the CPPs and the phospholipid bilayer, which is a prerequisite for the CPP translocation across the bilayer (Gao et al. 2019; Dunkin et al. 2011).

With the growing use and development of CPPs, there is a need to better understand the processes and energetics involved in the different uptake mechanisms, which may allow for development of more efficient delivery systems and de novo design of peptides with higher uptake. In this study we present an in-depth investigation of a single step in this process, the approach and interaction of CPPs with a model cell membrane. We investigate the penetration of seventeen peptides spanning the cationic, hydrophobic and amphipathic classes, using both Coarse-grained and all-atom molecular dynamics simulations. The use of computer simulations allows us to strictly control the composition and conditions of the systems, and analyze interactions and results with molecule level resolution.

This work only studies individual peptides, which give insight into the passive translocation behaviour of peptides at very low concentrations. However, the generated free energy profiles indicate that the behavior of the peptide is strongly dependent on the amino acid sequence, with single peptides showing free energy barriers towards passive diffusion to the center of the bilayer. However, adsorption onto the bilayer surface seems to be generally favorable for both amphipathic and hydrophobic peptides, perhaps paving the way for multiple peptides to translocate, synergistically. Further investigation into the interaction of CPPs at the bilayer membrane, and the energetics of multiple peptides are required to further investigate and understand these complex and interesting systems.

Methods

Based on physicochemical properties, seventeen peptides were selected for the study. Sequences of the CPPs (see Table 1) were taken from the Protein Data Bank, with two ends of each peptide being respectively terminated with -NH2 and -COOH groups. Generation and structure prediction of the CPPs were carried out using PEP-FOLD online server (Shen et al. 2014). Resultant structures were used to build reference coarse grained structures.

Coarse-Grained Molecular Dynamics Simulations

Coarse-grained molecular dynamics (CGMD) simulations were performed using the GROMACS (version 5.1.2) (Van Der Spoel et al. 2005) with the MARTINI force field (Marrink et al. 2007). Trajectories were visualized using the Visual Molecular Dynamics (VMD) software (Humphrey et al. 1996).

Initial peptide structures were first minimized and equilibrated in an aqueous solution. Then the full system was assembled, minimized and equilibrated for 10 ns in isothermal-isobaric prior to production runs. The leap-frog algorithm was used to evolve system coordinates with a timestep of 0.02 ps. The Berendsen thermostat was used to maintain a temperature of 300 K, while the Berendsen barostat was used to maintain pressure at 1 atm with the semi-isotropic pressure coupling; with cell fluctuations constrained in the directions parallel to the bilayer (x, y directions). Periodic boundary conditions were imposed on the x, y, z axes. The van der Waals interaction cut-off was 1.2 nm. The Particle Mesh Ewald (PME) method was used to calculate the long-ranged full electrostatic interactions.

A model membrane system of Dioleoylphosphatidylcholine (DOPC) lipid bilayer was generated with the MARTINI force field for lipids (Wassenaar et al. 2015). Peptide and the membrane were arranged in a periodic box with dimensions of $16 \times 16 \times 14$ nm and solvated with water using the MARTINI water model (Fig. 1). This resulted in a system with 882 lipid molecules (441 per leaflet). Na^+ and Cl^- ions were added in sufficient amounts to balance the charge and obtain an ionic strength of 0.15 $moldm^{-3}$. In the initial configuration, the peptide was positioned in water, such that the perpendicular separation of the peptide center-of-mass and bilayer is no less than ~ 4.7 nm. The water solution was assumed at pH = 7, with neutral DOPC.

Free Energy Profiles/Potential of Mean Force (PMF) Calculation

We performed umbrella sampling simulations to determine the PMF for a peptide translocating through a DOPC membrane. The reaction coordinate (ξ) was the z-component of the vector between the center of mass (COM) of the peptide and the COM of the lipid bilayer. The range of ξ sampled was from 0 to over 4.5 nm, i.e., when the peptide is in the middle of the bilayer to when the peptide is in bulk water. For the PMF calculations, the system underwent both the pulling processes and the equilibrium MD processes. A series of initial configurations were

Table 1 List of CPPs included in the study

Peptide name/Origin	Amino acid sequence	Resi-dues	Nominal charge
Cationic cell penetrating peptides			
Penetratin (Joliot et al. 1991; Derossi et al. 1994)	RQIKIWFQNRRMKWKK	16	+7 (0.44)
HIV-TAT (47–57) (Chem 1997; Ignatovich et al. 2003)	YGRKKRRQRRR	11	+8 (0.72)
R10 (S. 2013) (Futaki et al. 2001)	RRRRRRRRRR	10	+10 (1)
CCMV-Gag (7–25) (Chem 1997; Munyendo et al. 2012)	KLTRAQRRAAARKNKRNTRGC	21	+9 (0.43)
Chimeric dermaseptin S4 and SV40 'S413-PV'(Trabulo et al. 2010; Padari et al. 2010)	ALWKTLLKKVLKAPKKKRKVC	21	+9 (0.43)
Amphipathic cell penetrating peptides			
Transportan (Elmquist et al. 2001)	GWTLNSAGYLLGKINLKALAALAKKIL	27	+4 (0.15)
pVEC (vascular endothelial cadherin; Elmquist et al. 2001, 2006)	LLIILRRRIRKQAHAHSK	18	+6 (0.33)
MPG (Elmquist et al. 2006; Morris et al. 1997)	GALFLGFLGAAGSTMGAWSQPKKKRKV	27	+5 (0.16)
CADY/Chimeric peptide PPTG1 (Palm-Apergi et al. 2009)	GLWRALWRLLRSLWRLLWRA	20	+5 (0.25)
sC18 (Palm-Apergi et al. 2009)	GLRKRLRKFRNKIKEK	16	+8 (0.50)
C6 (Hoyer et al. 2012)	RLLRLLLRLWRRLLRLLR	18	+7 (0.39)
Hydrophobic cell penetrating peptides			
K-FGF (Kaposi's sarcoma fibroblast growth factor) (Jafari et al. 2013)	AAVALLPAVLLALLAP	16	0 (0)
Integrin β3-fragment (Wrighton et al. 1996; Liu et al. 2002)	VTVLAGALAGVGVG	14	0 (0)
Hepatitis B virus translocationmotif (Zhang et al. 1998)	PLSSIFSRIGDP	12	0 (0)
Grb2 (SH2 domain) (Bleifuss et al. 2006)	AAVLLPVLLAAP	12	0 (0)
Fusion sequence HIV-1gp41 (1–23) (Derossi et al. 1994; Rojas et al. 1998)	GALFLGFLGAAGSTMGA	17	0 (0)
C105Y (Morris et al. 1999)	CSIPPEVKFNKPFVYLI	17	+1 (0.06)

Amino acids are coloured according to their charge and hydrophilicity. Color code: Arg-R (blue), Lys-K (cyan), Tyr-Y (pink), Glu-E (red), Trp-W (green), Asp-D (orange), Neutral amino acids (gray)

generated via pulling the peptide into the membrane with a constant force of 1000 kJ. After a short NPT equilibration run for each configuration, MD run of 50 ns was performed with a harmonic bias potential with spring constant 1000 kJ mol^{-1} nm^{-2} on the peptide. Free-energy profiles were recovered using the Weighted histogram analysis method (WHAM) (Kästner 2011).

All-Atom Molecular Dynamics Simulations

Among the seventeen peptides, six peptides were selected for all atom simulations. All simulations were performed in GROMACS (version 5.1.2) using GROMOS96 53A6 force field. The simulation system includes 128 DOPC lipids (64 per leaflet) and a single CPP. The system is solvated in water. Na^+ and Cl^- ions were added to balance the charge and obtain an ionic strength of 0.15 mol dm^{-3}. We used periodic boundary conditions and the overall temperature of the system was kept constant. Each group of molecules were connected independently with the Berendsen thermostat of 300 K. The pressure is coupled to a Berendsen barostat at 1 atm separately in every dimension. The average cell dimensions are approximately $6 \times 6 \times 10$ nm. The integration of the equations of motion is performed using a leapfrog algorithm with a time step of 2 fs. This wide time step is possible by constraining the length of bonds involving hydrogen. A cut-off of 1.0 nm was applied to Lennard–Jones interactions.

Hydrogen Bonding

Hydrogen bonds were analysed through the built-in VMD plugin HBonds (version 1.2). The presence of an H-bond was based on geometry-based criteria, where distance between possible donor and acceptors was less than 3 Å and angle less than 20°. The -OH and $-NH_2$ groups were regarded as donors while O was always considered as an acceptor. H-bonds were counted throughout simulations and mean values reported.

Results

The focus of this study was to study the energetics of CPPs approaching a DOPC lipid bilayer. Although CPPs have been reported on widely, most studies focused on a single

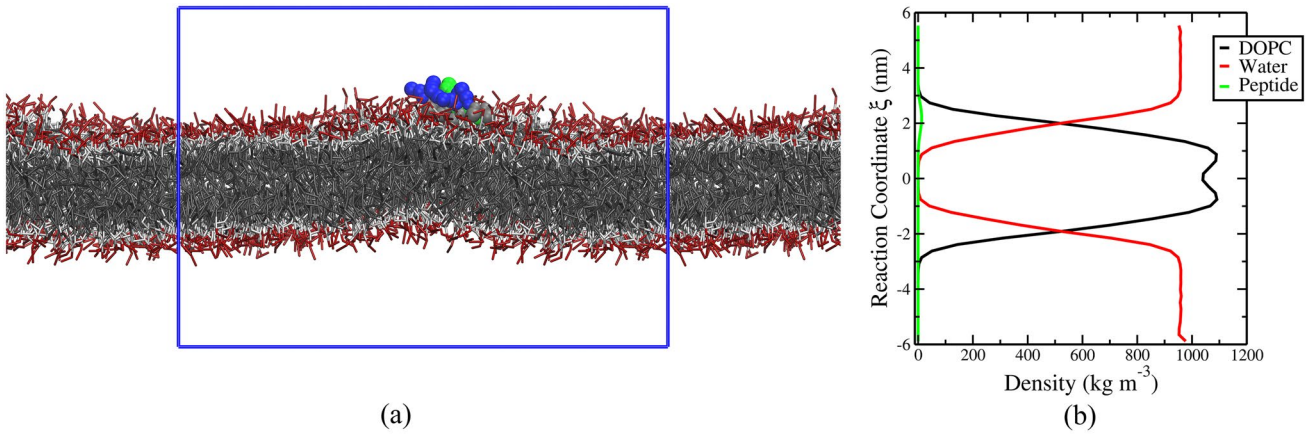

Fig. 1 **a** A snapshot from a MD trajectory with C6 peptide in contact with zwitterionic DOPC membrane. The simulation cell is denoted by the blue box, while periodic images are shown to either side. The peptide is shown using spheres where Lys amino acid residues are represented in cyan and Arg in blue. Lipids are represented with stick models, where the alkaline chain is gray, and the head group is in red. **b** Ensemble averaged density profiles of water molecules, DOPC molecules and the peptide along the reaction coordinate (ξ). The ξ value where the densities of water and the bilayer cross are considered as the surface of the bilayer (Color figure online)

CPP type and comparing results among studies is difficult due to the varying conditions used. Moreover, the possibility of several uptake mechanisms, unknown effects of peptide concentration at the bilayer, interaction of peptides with each other at the surface, and the convolution of multiple peptide interactions with the membrane are all factors which complicate the analysis of experimental results.

To better understand the guiding principles of CPP localization and uptake into cells, a systematic approach needs to be taken by eliminating as many variables as possible. In this study we focus on one specific aspect, namely the free energy profiles of single peptides approaching a neutral lipid bilayer membrane. This is a first step in understanding more complex behaviour, and eventually contextualizing experimental data.

Sequence Motifs and Structural Features of the Selected Peptides

CPPs can be classified as cationic, amphipathic and hydrophobic based on their physicochemical properties. While cationic and hydrophobic CPPs comprise a high proportion of positively charged, and apolar amino acid residues, respectively, amphipathic peptides present sequential assembly of hydrophobic and hydrophilic domains.

Five cationic CPPs, six amphipathic and six hydrophobic peptides were selected. These represent some of the most frequently investigated CPPs. In a previous study we have investigated the packing of these peptides to form siRNA-peptide complexes (Rathnayake et al. 2017). In this study, the main focus was to uncover sequence motifs and structural features which enhance adsorption and insertion. Details of the studied peptides are given in Table 1.

The Effective Interaction Between the Peptide and the Membrane

Free energy profiles (PMF) for insertion of peptide into the lipid bilayer were generated for all 17 CPPs, using Coarse-grained (CG) simulations. The minimum of the profile, ΔG_{min}, gives the energy cost of bringing the peptide from the bulk solution to its most favored displacement from the membrane surface. The free energy barrier for spontaneous and passive translocation (ΔG_{Trans}) is the energy difference between the CPP being located at the center of the bilayer ($\Delta G_{\xi=0}$) and the free energy minima (ΔG_{min}). In the following sections, the free energy profiles of hydrophobic, cationic and amphipathic peptides are discussed separately.

We also performed all-atom simulations to explicitly examine atomic interactions which are only indirectly accounted for in the coarse-grained simulations. In each section we will discuss experimental findings to give context to the energetics, as well as any pertinent observations uncovered by the atomistic simulations.

Profiles of Hydrophobic CPPs and the Hydrophobic Effect

Six hydrophobic CPPs were included in the study (see Table 1). K-FGF and Grb2 consist of only non-polar residues whereas, β3 and HIV-1-gb41 consist of both polar residues and non-polar residues, and Hep-B and C105Y consist of polar, apolar, positively charged and negatively charged residues. Due to the major non-polar portion, these CPPs can be expected to possess a high affinity for the hydrophobic domain of the lipid bilayer membrane. The representation of the secondary structure of peptides mapped onto the

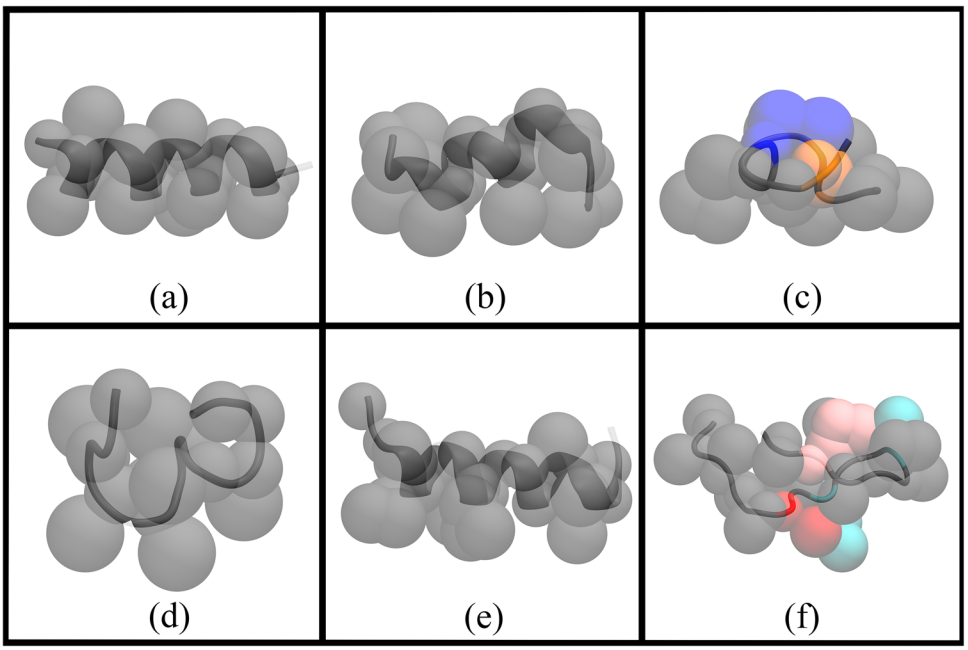

Fig. 2 Representation of the secondary structure of peptides mapped onto the coarse grained beads. **a** K-FGF **b** Integrin β3 **c** Hepatitis B **d** Grb2 **e** HIV-1gp41 **f** C105Y43. Color code as in Table 1: Arg-R (blue), Lys-K (cyan), Tyr-Y (pink), Glu-E (red), Trp-W (green), Asp-D (orange), Neutral amino acids (gray) (Color figure online)

coarse-grained beads is illustrated in Fig. 2 with the respective color codes.

Umbrella sampling simulations were performed, and the free energy profiles, which in this case are potential of mean force plots, were generated using the WHAM method. The free energy profiles and some representative snapshots for a hydrophobic peptide are shown in Fig. 3.

From the profiles shown in Fig. 3a, it is clear that beyond ξ ~ 3 nm, the peptides are in a bulk water environment, and show free movement without any interaction with the membrane. When the hydrophobic peptides begin to approach and interact with the membrane, the free energy change becomes negative, indicating that hydrophobic CPPs can spontaneously associate with the bilayer surface. Free energy profiles reach minima between ξ ~ 1.2 nm and 1.8 nm. Past these points, the ΔG increases again as CPPs reach the center of the bilayer (ξ = 0).

The energy profiles of hydrophobic CPPs can be explained through the hydrophobic effect. When small hydrophobic peptides are placed in an aqueous medium, the transient hydrogen bond networks between water molecules are disrupted to make room for the hydrophobe. These broken H-bonds are not replenished, leading to an endothermic solvation process. Moreover, it is thought water bonds distort to form ice-like cage structures called 'clathrate cages' around the hydrophobe, leading to lowering of entropy. Conversely, association of two nonpolar molecules reduces the total nonpolar surface area exposed, thus reducing the amount of structured water and providing a favorable entropy of association. This effectively attracts the hydrophobic CPP onto the surface of the membrane.

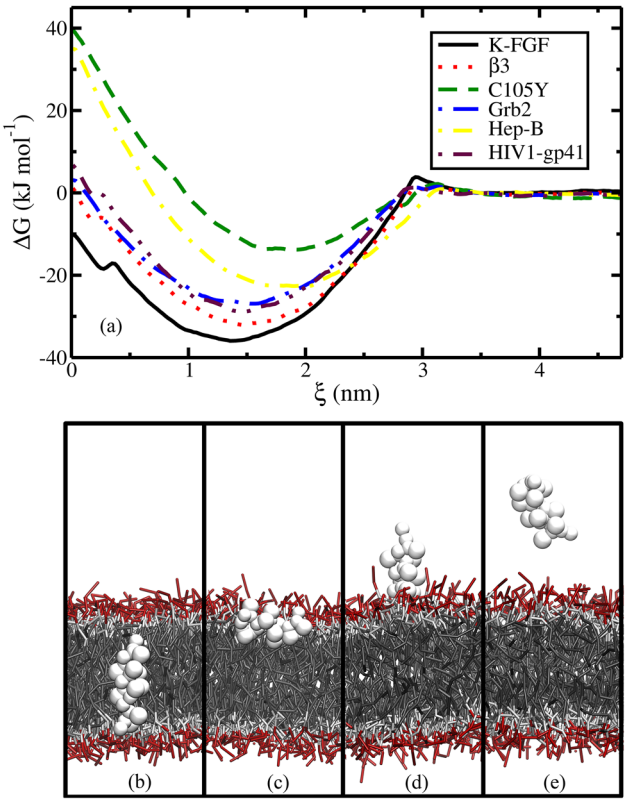

Fig. 3 **a** Free energy profiles for Hydrophobic cell-penetrating peptides K-FGF, β3, C105Y, Grb2 Hep-B and HIV1-gp41(top). **b–e** Snapshots of the hydrophobic CPPs K-FGF at different ξ points along the free energy profiles. **b** ξ = 0.1 nm, **c** ξ = 1.5 nm **d** ξ = 3.0 nm **e** ξ = 4.7 nm (bottom). The peptide has been shown in front of the bilayer and water molecules were hidden for clarity

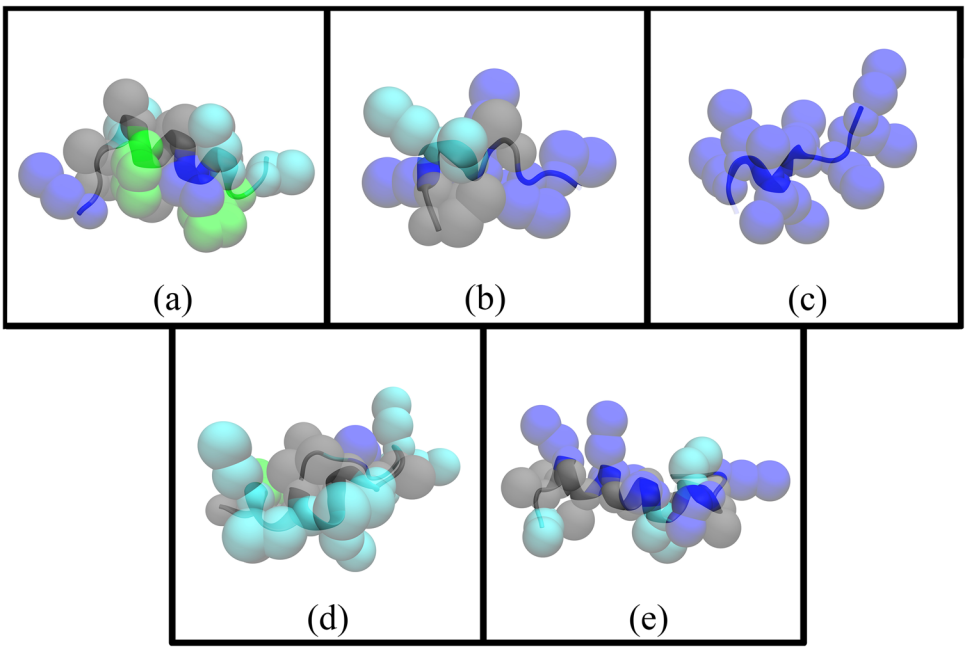

Fig. 4 Representation of the secondary structure of peptides mapped onto the coarse grained beads. **a** Penetratin **b** HIV-TAT **c** R10 **d** SV40 **e** CCMV-Gag. Color code: Arg-R (blue), Lys-K (cyan), Tyr-Y (pink), Glu-E (red), Trp-W (green), Asp-D (orange), Neutral amino acids (gray) (Color figure online)

Considering the different hydrophobic peptides, the shape of profiles is related to the total charge, with the neutral K-FGF, Grb2, β3 and HIV-1-gp41 showing similar profiles, while charged Hep-B and C105Y show free energy profiles with cationic character (see Fig. 5 and relevant discussion). According to the translocation free energy barrier values K-FGF shows the lowest value of 26.0 kJ mol^{-1}. Moreover, this peptide shows a free energy minimum at $\xi_{min} = 1.42$ nm, where the COM is almost past the head group of the lipid bilayer. K-FGF consists exclusively of nonpolar amino acid residues with a high number of Ala and Leu. Although K-FGF does not spontaneously pass through the membrane bilayers, it is partially inserted into the bilayer and partially exposed to the solvent. Grb2 shows the second lowest ΔG_{Trans} value of 30.0 kJ mol^{-1}. The composition of Grb2 is similar to K-FGF except it has only 12 amino acid residues compared to 16 residues in K-FGF. Integrin-β3 and Fusion sequence HIV-1gp41 show translocation free energies of 33.8 kJ mol^{-1} and 35.5 kJ mol^{-1}, respectively. Both peptides contain around 60% hydrophobic residues. However, Integrin-β3 consists of polar amino acid Thr and Fusion sequence HIV-1gp41 consists of polar amino acids Thr and Ser. These peptides show a similarity in translocation free energy profiles. Hep-B and C105Y show the highest translocation free energy barrier values of 57.6 kJ mol^{-1} and 53.1 kJ mol^{-1}, respectively.

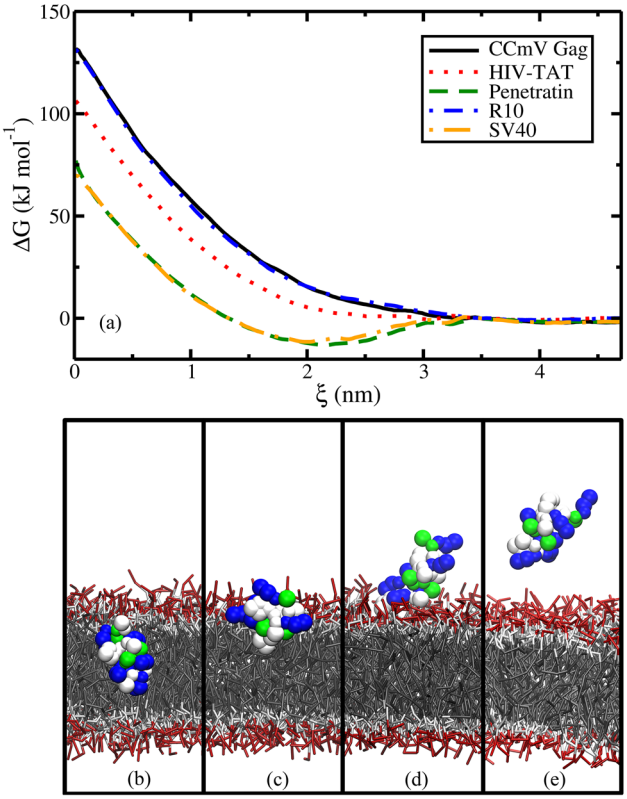

Fig. 5 **a** Free energy profiles for cationic cell-penetrating peptides Penetratin, HIV-tat, R10, CCMV-gag and SV40 (top). **b**–**e** Snapshots of the cationic CPP penetratin at different ξ points along the free energy profiles (bottom). **b** ξ = 0.1 nm, **c** ξ = 1.5 nm **d** ξ = 3.0 nm **e** ξ = 4.0 nm. The peptide has been shown in front of the bilayer and water molecules were hidden for clarity

Profiles of Cationic CPPs; the Impact of Electrostatics and Solvation

Most peptide sequences identified as CPPs are polycationic at physiological pH. In our study, we have modelled some

widely investigated cationic CPPs including Penetratin, HIV-tat, R10, CCMV-gag and SV40. The representation of the secondary structure of peptides mapped onto the coarse-grained beads is illustrated in Fig. 4.

Figure 5 presents the free energy profiles of translocation for the selected cationic CPPs. The overall shape of the PMF is roughly repulsive for all cationic CPPs, with a sharp maximum at $\xi = 0$. For three of the peptides (CCmV GAg, R10, HIV-TAT) these profiles are monotonously repulsive, while for two peptides (SV40, Penetratin) a broad, shallow minimum exists, corresponding to where the peptide is interacting favourably with the bilayer.

When approaching the DOPC membrane from bulk water, progressively increasing coulombic repulsion and desolvation occurs. Smaller attractive forces arise from the non-bonded interactions the peptide forms with the bilayer molecules, and the soft hydrophobic effect in play with any non-polar residues of the peptide. Although some of the cationic CPPs will show some adsorption prevalence, the free energy barrier for spontaneous passive diffusion is very large, i.e., between ~ 80 and 140 kJ mol^{-1}. This energy barrier cannot be overcome by thermal vibrations, and the possibility of a peptide approaching the center of the membrane is low, in the time scales that we have sampled.

This result may seem to contradict previous reports, where cationic peptides have been shown to translocate the membrane. However, a few reasons may explain this apparent inconsistency. Firstly, the charge on the bilayer may have a large effect. It is known that surface accumulation of purely cationic peptides, such as R10, TAT and CCMV Gag is strongly driven by electrostatics and is more sensitive to the pH of the medium and the content of acidic lipids in the target membrane. Indeed, these peptides are deactivated under acidic conditions as they do not bind to a neutral membrane (Ramírez et al. 2020). Furthermore, the unfavourable energetics of transfer have been reported (Almeida 2014). Secondly, the presence of several peptides on the membrane may completely change the energetics of translocation. In fact, the proposed mechanisms of the entry of cationic CPPs rely on group action of peptides rather than the entry of individual peptides. Studies on living cells show that the uptake of arginine-rich peptides could be a combination of both direct translocation and endocytosis (Ruseska and Zimmer 2020). It has also shown that the switch between different uptake mechanisms might be concentration-dependent. At low concentration, cationic CPPs are found to be mainly endocytosed, whereas rapid cytoplasmic entry occurred at higher concentration (Ruseska and Zimmer 2020).

Although the translocation processes for the five peptides were similar at the early stage, the charge and hydrophobicity of different peptides does affect their interactions with lipids especially after the insertion into the bilayer.

Experimentally, it has been reported Arginine residues are more effective for internalization than Lysine, and this efficiency is attributed to the guanidinium headgroup of the arginine side chain rather than to the positive charge alone (Sagan 2013; Dunkin et al. 2011). The guanidinium group forms bidentate hydrogen bonds with negatively charged phosphate, sulfate and carboxylate groups on the cell surface. This was also qualitatively observed in the all-atom simulations performed by us. Polyarginines are one of the most studied CPPs in terms of mechanism of internalization. Subsequently, it has been noted that the efficiency with which linear polyarginines are taken up differs depending on sequence length and on the number and position of arginine residues in the sequence. The impact of aromatic amino acids on the interaction of CPPs with lipid membranes has also been the subject of many studies. Trp, in particular, seems to bind strongly to the membrane lipids' carbonyl groups. For example, Trp end-tagging improves the adsorption of arginine-rich CPPs to melanoma cells over non-malignant cells (Ramírez et al. 2020; Rydberg et al. 2012).

Distribution of cations among anionic and hydrophobic residues is key for Penetratin permeation (Carrigan and Imperiali 2005). A notable feature is that the free energy barrier to translocation is consistently lower in the case of Penetratin than that for the TAT peptide, which is also supported by the literature (Yesylevskyy et al. 2009). We observe (through all atom simulations) that the Arg and Lys side chains on the TAT peptides bind to the zwitterionic phospholipid phosphate and carbonyl groups and occupy a region beneath the phosphate groups at the interface, with the carbon chains of the phospholipids. However, we were not able to observe a spontaneous penetration of either Penetratin or the TAT peptide on the time scale of the simulations. Both peptides appeared to diffuse randomly on the surface of the membrane and showed little tendency to penetrate the membrane. Research shows that TAT peptides at high concentrations translocate across membranes via a transient water pore at longer time scales (Herce and Garcia 2007).

Amphipathic CPPs; the Correlation of the Secondary Structure with Membrane Interaction

We have modelled a set of six amphipathic CPPs, namely; C6, CADY, MPG, pVEC, sC18 and Transportan. These peptides have both hydrophobic regions and hydrophilic regions, and consequently are generally longer. The representation of the secondary structure of peptides mapped onto the coarse-grained beads are illustrated in Fig. 6 with respective color codes.

The free energy profiles calculated for the amphipathic peptides are shown in Fig. 7. As would be expected, the

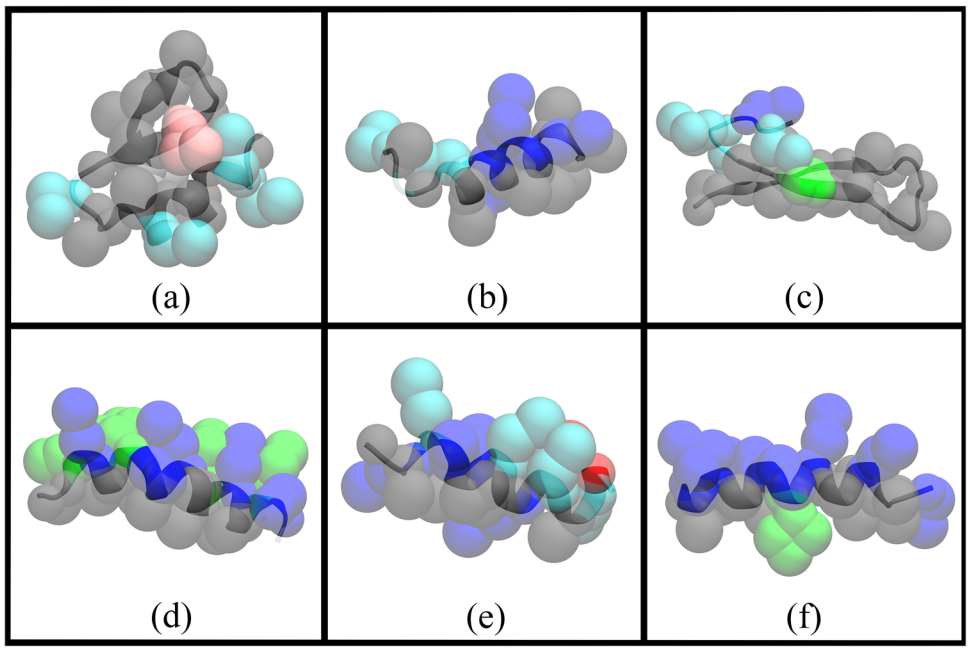

Fig. 6 Representation of the secondary structure of peptides mapped onto the coarse grained beads. **a** Transportan **b** pVEC **c** MPG **d** CADY **e** sC18 **f** C6. Color code: Arg-R (blue), Lys-K (cyan), Tyr-Y (pink), Glu-E (red), Trp-W (green), Asp-D (orange), Neutral amino acids (gray) (Color figure online)

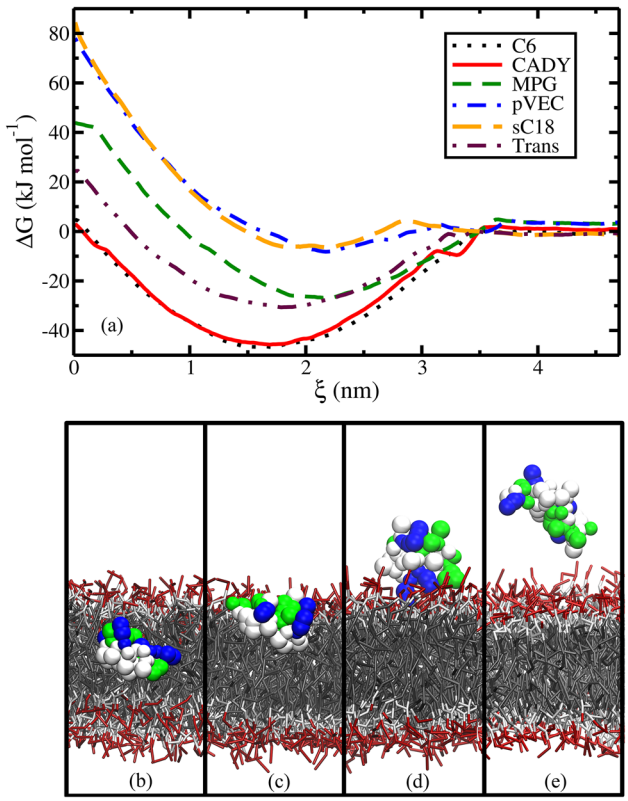

Fig. 7 **a** Free energy profiles for amphipathic cell-penetrating peptides C6, CADY, MPG, pVEC, sC18 and Transportan (top). **b–e** Snapshots of the amphipathic CPP C6 at different ξ points along the free energy profiles. **b** ξ = 0.1 nm, **c**, ξ = 1.5 nm **d** ξ = 3.0 nm **e** ξ = 4.7 nm. The peptide has been shown in front of the bilayer and water molecules were hidden for clarity

profiles show features of both hydrophobic and cationic peptides. The free energies decrease and become negative at the vicinity of the bilayer surface. They reach minima around 2.0 nm and then gradually increase as the peptides reach the center of the bilayer, where the PMF acquires a high positive value.

All of the peptides show negative adsorption free energy profiles, indicating that the peptides are attracted to the membrane and prefer to stay adsorbed on the surface of the cell membrane. Generally, the adsorption is favored by hydrophobicity. However, the translocation free energy barrier is largely positive. Thus, there will be no spontaneous translocation through the bilayer.

Both C6 and CADY peptides have amphipathic α-helix structures, in which hydrophilic and hydrophobic amino acids are grouped in separate faces of the helix. All-atom simulations also showed C6 peptides had random orientations in bulk water, but the hydrophobic face of C6 was oriented towards the membrane. This clearly indicates the importance of hydrophobic interactions in membrane translocation. Moreover, both peptides contain aromatic membrane binding residues. These factors may result in these peptides in showing the strongest adsorption to the bilayer.

Another example of how the secondary structure of amphipathic peptides is strongly correlated with bilayer interaction is through Transportan. This peptide adopts a helical structure, with the 4–12 residues region maintaining α- helix and the terminal with antiparallel β-sheet hairpin structure. The charged amino acids point outwards from both sides of the bent molecule, facilitating the binding of the peptide to the charged surface of the lipid membrane.

The free energy profiles for Transportan, C6 and CADY show similar forms (see Fig. 7), and they exhibit close free energies of absorption of 55.9 kJ mol^{-1}, 49.5 kJ mol^{-1} and 51.5 kJ mol^{-1}, respectively. These peptides also share sequence composition; all three have charged, polar and apolar residues. The free energy minimum is found at the surface of the bilayer ($\xi = 2$ nm) for these peptides. When the peptide moves through the bilayer towards the COM of the bilayer, the free energy gradually increases and becomes positive. This seems to be due to the presence of positively charged groups, which make strong interactions with water and prefer the aqueous environment.

The free energy profiles for pVEC and sC18 are similar. Both consist of cationic residues, and sC18 has a negatively charged residue in the peptide as well. Due to the presence of charged particles the free energy plots resemble those of cationic peptides.

Hydrogen Bonding Analysis

From trajectories of all-atom simulations, the hydrogen bonds formed by the peptides were compared; both in the vicinity of the bilayer (adsorbed) and removed from it (free). Atomistic simulations were run for 6 peptides: Penetratin, SV40 peptides K-FGF, C6, Transportan and Fusion sequence HIV-1gp41. Table 2 lists the average H-bonds formed for peptides, in both states. The H-bonds are categorized as those involved in (1) intramolecular bonds, and intermolecular bonds between (2) the peptide and the bilayer, and (3) the peptide and water.

An expected lowering of the number of h-bonds with water, when the peptide is absorbed, was observed. Interestingly, the intramolecular H-bonding affinity for the peptides when adsorbed onto the bilayer surface decreases for cationic peptides, but increases for both other classes. This may indicate a stronger secondary structure for these peptides at the interface. Moreover, when considering the total number of intermolecular H-bonds formed by the peptides, the cationic CPPs seem to have a net gain through the process of adsorption, while both other classes incur loss. This is contrary to the free energy profiles, and indicates the domination of the solvation effects and entropy in this adsorption process.

Bidentate hydrogen bonds formed between guanidinium-rich peptides and H-bond acceptors on the cell surface have previously been demonstrated to be important for efficient membrane interaction and cellular uptake (Guidotti et al. 2017; Borrelli et al. 2018). The formation of bidentate H-bonds with the membrane were observed in the all-atom trajectories. Both the Lysine (pKa ~ 10.5) and Arginine (pKa of ~ 12.5) are fully protonated under physiological conditions, allowing for the formation of H-bonds. However, the arginine residues also possess a delocalized positive charge in the guanidinium group that enables formation of an ion pair or even coordinated bidentate H-bonds with anionic membrane constituents, which promote its adsorption onto membranes. The presence of guanidinium groups in cationic Penetratin and SV40 resulted in a much higher adsorption due to the ability of the former to make strong bidentate H-bonds with various anions such as the phosphate head groups of the membrane lipids. Hydrophobic CPPs, formed the least number of H-bonds with respect to cationic and amphipathic peptides. This indicates that the number of hydrogen bonding sites on the peptides might be an important factor for the interaction between the peptides and lipid membranes, as well as for their cellular uptake. Thus, the calculated degree of hydrogen bonding with water reflects the measured adsorption onto lipid membranes, suggesting the latter involves hydrogen bonding with the lipid head groups.

General Outlook, Limitations and Future Directions

The aim of this study was to provide identical conditions to a series of cell penetrating peptides in the vicinity of a neutral lipid bilayer, allowing us to objectively compare their energetics. This can be considered a small, but essential step in

Table 2 The number of hydrogen bonds formed by peptides with different components while in adsorbed and free states

Peptide	Class	Average H-bonds peptides form				
		Intramolecular		With water		With Bilayer
		(Adsorbed)	(Free)	(Adsorbed)	(Free)	(Adsorbed)
Penetratin	Cationic	2.20 ± 1.40	2.63 ± 1.40	12.10 ± 3.12	13.22 ± 3.21	3.93 ± 1.40
SV40	Cationic	2.00 ± 1.23	2.00 ± 1.20	8.20 ± 2.59	14.64 ± 1.30	9.10 ± 2.40
Transportan	Amphipathic	4.65 ± 1.70	3.41 ± 1.62	10.14 ± 2.67	17.39 ± 3.80	7.00 ± 1.80
C6	Amphipathic	3.91 ± 1.75	2.45 ± 1.42	9.35 ± 2.78	11.42 ± 3.12	1.97 ± 1.41
HIV-1gp41	Hydrophobic	2.25 ± 1.30	1.44 ± 1.14	5.56 ± 2.12	10.80 ± 3.80	2.57 ± 1.36
K-FGF	Hydrophobic	2.75 ± 1.37	1.65 ± 1.20	5.34 ± 2.00	7.60 ± 3.00	1.34 ± 1.02

*Standard deviation of the measurement has been given as the uncertainty

Table 3 Summary of free energy changes for the selected cell-penetrating peptides

Peptide name/Origin	$\Delta G(\xi_{min})$/kJ mol^{-1}	ξmin nm	$\Delta G(0)$/kJ mol^{-1}	$\Delta G_{Trans} = \Delta G(0) - \Delta G(\xi_{min})$/kJ mol^{-1}
Cationic cell penetrating peptides				
Penetratin	− 13.6	2.12	76.6	90.2
HIV-TAT (47–57)	− 1.10	3.06	105	106
R10	0.00	3.67	131	131
CCMV-Gag (7–25)	0.00	3.84	131	131
Chimeric dermaseptin S4 and SV40 'S413-PV'	− 11.8	2.01	70.0	81.8
Amphipathic cell penetrating peptides				
Transportan	− 31.2	1.80	24.7	55.9
pVEC (vascular endothelial cadherin)	− 8.40	2.20	76.3	84.7
MPG	− 27.3	2.13	43.5	70.8
CADY/Chimeric peptide PPTG1	− 46.4	1.68	3.10	49.5
sC18	− 6.5	1.81	83.7	90.2
C6	− 47.4	1.70	4.10	51.5
Hydrophobic cell penetrating peptides				
K-FGF (Kaposi's sarcoma fibroblast growth factor)	− 36.2	1.42	− 10.1	26.0
Integrin β3-fragment	− 32.9	1.44	0.90	33.8
Hepatitis B virus translocation motif	− 13.9	1.70	39.8	53.6
Grb2 (SH2 domain)	− 26.8	1.57	3.20	30.0
Fusion sequence HIV-1gp41 (1–23)	− 22.9	1.46	34.7	57.6
C105Y	− 13.6	1.92	39.5	53.1

understanding the processes involved in the passive uptake pathways of peptides.

Significant points in the free energy profiles of the CPPs are free energy change ($\Delta G(\xi_{min})$) and location (ξ_{min}) of the minima, the energy at the bilayer center ($\Delta G(0)$), and the barrier for translocation (ΔG_{Trans}). Table 3 lists these extracted values, summarizing our findings.

Hydrophobic peptides show the strongest adsorption and are located almost entirely in the interfacial region, with large barriers to move to the center of the bilayer. However, in real systems, it may be entirely possible that hydrophobic peptides would not approach a cell membrane in this form, and peptide-peptide interactions may play a large role in the process. Moreover, the strong adsorption of these peptides might be a disadvantage considering the release into the cytosol, if other mechanisms are in play to flip the inner and outer bilayer leaflets.

Cationic CPPs show only moderate adsorption capacity, while having a repulsive profile within the bilayer. However, it should be noted that most cell membranes have a slight net negative charge, and coulombic interactions would have a much longer range that the vdW and hydrophobic interactions which dominate in our simulations. This long-ranged attraction may allow cationic peptides to concentrate in the region above the membrane, where many other mechanisms may initiate.

As expected, amphipathic peptides present properties of both hydrophobic and cationic peptides, but in our studies, the importance of membrane-binding aromatic amino acids, and the importance of secondary structure was observed acutely. Moreover, the ability to tune the long-ranged attraction and membrane interaction and binding imbue the amphipathic peptides with the most engineering flexibility, and may be the most promising class for de novo peptide design.

Although numerous peptides have been shown to promote uptake and translocation, there has been no comprehensive comparison of individual peptide performance under standardized conditions. In most experimental studies, the peptides investigated are not compared to other CPPs under identical conditions. Therefore, we wanted to devise a method using a defined, reproducible system that would permit the comparison and ranking of a range of CPPs. We have ranked the CPPs belonging to each class to identify the most effective CPPs for a given transport task. Among the 17 CPPs we have chosen, only few CPPs have been evaluated using wet lab experiments.

Among the cationic peptides, the best performers were Penetratin, Transportan and R10 which is also confirmed by experimental results (Ramaker et al. 2018). An explanation for the more effective uptake of positively charged CPPs may lie in the existence of negatively charged proteoglycans and

phospholipids on the cell surface that enable an electrostatic interaction between positively charged CPPs and the membrane as first step for internalization, followed by endocytic pathways or direct translocation (Bechara and Sagan 2013).

Our findings show that Transportan and C6 are the best amphipathic CPPs for passive translocation. There is experimental evidence to prove the insertion of Transportan into hydrophobic core and cross the phospholipid membranes (Langel 2021). However, no wet lab experiments were performed on synthetic C6 CPPs to demonstrate their delivery kinetics. CADY, MPG, pVEC and sC18 can be ranked from highest to the lowest according to their ability to translocate through bilayers, respectively. The affinity for phospholipids and internalization pathways for these CPPs has been tested using circular dichroism spectra (Eiríksdóttir et al. 2010) and have been already reported in the literature.

Our results are consistent with the fluorescence and circular dichroism (CD) spectroscopy studies of K-FGF (Ruzza et al. 2010), which could be summarized as follows: hydrophobic K-FGF, bind and insert into lipid vesicles predominantly via hydrophobic interaction between the lipid fatty acid acyl chains and the hydrophobic peptide segment, showing high affinity towards bilayers. Thus, K-FGF acts as the best hydrophobic CPP according to our study. The rest are in the order of Grb2, Integrin β-fragment, C105Y, Hepatitis B virus translocation motif and fusion sequence HIV-1gp41 (1–23) (Rhee and Davis 2006).

It should be noted that considering all of the above, it is certainly not possible to identify one 'ultimate' CPP for all purposes. Yet, a general trend for a 'good performer' in our set up can be deduced when comparing the characteristics of our top CPPs.

As mentioned, energy barriers for translocation were observed for all peptides and translocation was not observed for free MD simulations even of the order of 1 μs. We suggest that either these barriers have to be overcome by long time-scale events or that these free energy profiles change due to other physical conditions. Both aspects may be in play. The spontaneous translocation of the peptide across a membrane is known from experiment to be a rare process, with rates on the order of single events per minute.

It should be noted that the choice of including temperature, membrane composition and peptide concentration plays a huge role. The contribution of different lipids, head groups, membrane proteins or other constituents is too specific to rigorously study. The temperature of 300 K was made to compare our results with prior in vitro and in silico studies. However, the energetics at physiological temperatures (~ 310 K) may have an influence on the results.

The use of computational molecular dynamics simulations introduces some system uncertainties which need to be acknowledged, the foremost of these is that coarse-grained force fields affect the conformational space of the peptides, particularly the MARTINI force field which uses biased constraints for the secondary structure. However, atomistic simulations were performed on several chosen systems, to qualitatively measure the change of conformation with the environment, which was shown to be small.

Peptide-based drug design has gained renewed interest with the discovery of cell-penetrating peptides. Currently, CPPs are involved in a wide variety of biomedical applications including imaging; direct action as antimicrobials, antifungal and anti-parasitics; and also, as a carrier to deliver drugs, small interfering RNA (siRNA), nucleotides, proteins, and peptides. Understanding the translocation mechanism of these peptides and identifying the residues or elements that contribute to uptake can provide valuable clues toward the design of novel peptides. As per wet-lab experiments, identifying and validating CPPs which would embed itself into the membrane and facilitate the translocation of cargo is an extremely difficult task, because bio membrane penetration is a dynamic process, and it is very difficult to predict dynamic behavior of the peptide from a sequence alone. To avoid this difficulty, we have studied different classes of CPPs by analyzing the trajectories and translocation pathways of single peptide MD simulations. This is a crucial step in a computational pipeline to understand the CPP translocation in a thermodynamic perspective.

All data we have presented here are for the single peptide systems. A more complicated process involving synergism of peptides or a more complex bilayer structure could be implemented to reduce the free energy barrier of translocation and acquire a significant possibility of spontaneous translocation. Preliminary results on multiple peptide systems indicate that the peptides show strikingly different energy profiles, with considerably reduced energy barriers for translocation. These gaps in our understanding, such as the effect of physical conditions, membrane composition and peptide concentration require further study, to provide insights for experimental CPP research.

Conclusion

Cell penetrating peptides cover a wide range of physicochemical natures and understanding the structure–activity relationships of these molecules is key to harnessing their potential. In this work, we have applied molecular dynamics simulations to characterize the interaction between cell-penetrating peptides and DOPC lipid bilayer membranes. Through coarse-grained molecular dynamics simulations, we have constructed the free energy profiles of 17 different cell-penetrating peptides inserting into a bilayer. This is perhaps the widest study of CPPs with similar conditions.

Although most experimentally known CPPs are cationic, high positive charge resulted in repulsive free energy

profiles, indicating that the uptake of cationic peptides occurs through either endocytic pathways, or different system conditions, such as temperature, membrane tension and composition, and CPP concentration. Hydrophobic sequences tend to enhance adsorption, but the free energy minima of these peptides were also close to the bilayer interface, with significant free energy changes occurring when going from the surface to the bilayer center. Hydrogen bonds observed from all-atom simulations also confirmed the well-established significance of water structuring, secondary structure, and specific amino acid interactions in the association of peptides with the membrane.

Author Contributions Not applicable.

Funding Not applicable.

Data Availability All data used for this project are publicly available and accessible online. We have annotated the entire data generation process and empirical techniques presented in the paper. The datasets generated during and/or analysed during the current study are available in the [ZENODO] repository, DOI [https://doi.org/10.5281/zenodo.4922401].

Declarations

Conflict of interest Not applicable.

Ethical Approval Not applicable.

Consent to Participate Not applicable.

References

Agrawal P, Bhalla S, Usmani SS et al (2016) CPPsite 2.0: a repository of experimentally validated cell-penetrating peptides. Nucleic Acids Res. https://doi.org/10.1093/nar/gkv1266

Almeida PF (2014) Membrane-active peptides: binding, translocation, and flux in lipid vesicles. Biochim Biophys Acta - Biomembr 1838:2216–2227. https://doi.org/10.1016/j.bbamem.2014.04.014

Bechara C, Sagan S (2013) Cell-penetrating peptides: 20 years later, where do we stand? FEBS Lett 587:1693–1702. https://doi.org/10.1016/j.febslet.2013.04.031

Bleifuss E, Kammertoens T, Hutloff A et al (2006) The translocation motif of hepatitis B virus improves protein vaccination. Cell Mol Life Sci. https://doi.org/10.1007/s00018-005-5548-7

Borrelli A, Tornesello AL, Tornesello ML, Buonaguro FM (2018) Cell penetrating peptides as molecular carriers for anti-cancer agents. Molecules. https://doi.org/10.3390/molecules23020295

Carrigan CN, Imperiali B (2005) The engineering of membrane-permeable peptides. Anal Biochem 341:290–298. https://doi.org/10.1016/j.ab.2005.03.026

Chem JB (1997) Cell biology and metabolism : a truncated HIV-1 Tat protein basic domain rapidly translocates through the plasma membrane and accumulates in the cell nucleus A truncated HIV-1 Tat protein basic domain rapidly translocates through the plasma membrane and A. 272:16010–16017

Choe S (2020) Molecular dynamics studies of interactions between Arg9(nona-arginine) and a DOPC/DOPG(4:1) membrane. AIP Adv. https://doi.org/10.1063/5.0015665

Derossi D, Joliot AH, Chassaing G, Prochiantz A (1994) The third helix of the Antennapedia homeodomain translocates through biological membranes. J Biol Chem 269(14):10444–10450

Dunkin CM, Pokorny A, Almeida PF, Lee HS (2011) Molecular dynamics studies of transportan 10 (Tp10) interacting with a POPC lipid bilayer. J Phys Chem B 115:1188–1198. https://doi.org/10.1021/jp107763b

Eiríksdóttir E, Konate K, Langel Ü et al (2010) Secondary structure of cell-penetrating peptides controls membrane interaction and insertion. Biochim Biophys Acta - Biomembr 1798:1119–1128. https://doi.org/10.1016/j.bbamem.2010.03.005

Elmquist A, Lindgren M, Bartfai T, Langel Ü (2001) Ve-cadherin-derived cell-penetrating peptide, pVEC with carrier functions. Exp Cell Res 269:237–244. https://doi.org/10.1006/excr.2001.5316

Elmquist A, Hansen M, Langel Ü (2006) Structure-activity relationship study of the cell-penetrating peptide pVEC. Biochim Biophys Acta - Biomembr 1758:721–729. https://doi.org/10.1016/j.bbamem.2006.05.013

Futaki S, Suzuki T, Ohashi W et al (2001) Arginine-rich peptides. An abundant source of membrane-permeable peptides having potential as carriers for intracellular protein delivery. J Biol Chem 276:5836–5840. https://doi.org/10.1074/jbc.M007540200

Gao X, Hong S, Liu Z et al (2019) Membrane potential drives direct translocation of cell-penetrating peptides. Nanoscale 11:1949–1958. https://doi.org/10.1039/c8nr10447f

Gräslund A, Madani F, Lindberg S et al (2011) Mechanisms of cellular uptake of cell-penetrating peptides. J Biophys. https://doi.org/10.1155/2011/414729

Guidotti G, Brambilla L, Rossi D (2017) Cell-penetrating peptides: from basic research to clinics. Trends Pharmacol Sci 38:406–424. https://doi.org/10.1016/j.tips.2017.01.003

Herce HD, Garcia AE (2007) Molecular dynamics simulations suggest a mechanism for translocation of the HIV-1 TAT peptide across lipid membranes. Proc Natl Acad Sci U S A 104:20805–20810. https://doi.org/10.1073/pnas.0706574105

Hoyer J, Schatzschneider U, Schulz-Siegmund M, Neundorf I (2012) Dimerization of a cell-penetrating peptide leads to enhanced cellular uptake and drug delivery. Beilstein J Org Chem. https://doi.org/10.3762/bjoc.8.204

Humphrey W, Dalke A, Schulten K (1996) VMD: visual molecular dynamics. J Mol Graph 14:33–38. https://doi.org/10.1016/0263-7855(96)00018-5

Ignatovich IA, Dizhe EB, Pavlotskaya AV et al (2003) Complexes of plasmid DNA with basic domain 47–57 of the HIV-1 Tat protein are transferred to mammalian cells by endocytosis-mediated pathways. J Biol Chem 278:42625–42636. https://doi.org/10.1074/jbc.M301431200

Jafari M, Karunaratne DN, Sweeting CM, Chen P (2013) Modification of a designed amphipathic cell-penetrating peptide and its effect on solubility, secondary structure, and uptake efficiency. Biochemistry. https://doi.org/10.1021/bi4001326

Jobin ML, Vamparys L, Deniau R et al (2019) Biophysical insight on the membrane insertion of an arginine-rich cell-penetrating peptide. Int J Mol Sci. https://doi.org/10.3390/ijms20184441

Joliot A, Pernelle C, Deagostini-Bazin H, Prochiantz A (1991) Antennapedia homeobox peptide regulates neural morphogenesis. Proc Natl Acad Sci. https://doi.org/10.1073/pnas.88.5.1864

Kästner J (2011) Umbrella sampling. Wiley Interdiscip Rev Comput Mol Sci 1:932–942. https://doi.org/10.1002/wcms.66

Langel Ü (2021) Cell-penetrating peptides and transportan

Liu KY, Timmons S, Lin YZ, Hawiger J (2002) Identification of a functionally important sequence in the cytoplasmic tail of integrin beta 3 by using cell-permeable peptide analogs. Proc Natl Acad Sci. https://doi.org/10.1073/pnas.93.21.11819

Lundberg P, Langel U (2003) A brief introduction to cell-penetrating peptides. J Mol Recognit 16:227–233. https://doi.org/10.1002/jmr.630

Ma JL, Wang H, Wang YL et al (2015) Enhanced peptide delivery into cells by using the synergistic effects of a cell-penetrating peptide and a chemical drug to alter cell permeability. Mol Pharm 12:2040–2048. https://doi.org/10.1021/mp500838r

Marrink SJ, Risselada HJ, Yefimov S et al (2007) The MARTINI force field: coarse grained model for biomolecular simulations. J Phys Chem B. https://doi.org/10.1021/jp071097f

Morris MC, Vidal P, Chaloin L et al (1997) A new peptide vector for efficient delivery of oligonucleotides into mammalian cells. Nucleic Acids Res. https://doi.org/10.1093/nar/25.14.2730

Morris MC, Chaloin L, Méry J et al (1999) A novel potent strategy for gene delivery using a single peptide vector as a carrier. Nucleic Acids Res. https://doi.org/10.1093/nar/27.17.3510

Munyendo WLL, Lv H, Benza-Ingoula H et al (2012) Cell penetrating peptides in the delivery of biopharmaceuticals. Biomolecules 2(2):187–202

Padari K, Koppel K, Lorents A et al (2010) S413-PV cell-penetrating peptide forms nanoparticle-like structures to gain entry into cells. Bioconjug Chem. https://doi.org/10.1021/bc900577e

Palm-Apergi C, Lorents A, Padari K et al (2009) The membrane repair response masks membrane disturbances caused by cell-penetrating peptide uptake. FASEB J. https://doi.org/10.1096/fj.08-110254

Ragin AD, Morgan RA, Chmielewski J (2002) Cellular import mediated by nuclear localization signal peptide sequences. Chem Biol. https://doi.org/10.1016/S1074-5521(02)00189-8

Ramaker K, Henkel M, Krause T et al (2018) Cell penetrating peptides: a comparative transport analysis for 474 sequence motifs. Drug Deliv 25:928–937. https://doi.org/10.1080/10717544.2018.1458921

Ramírez PG, Del Pópolo MG, Vila JA, Longo GS (2020) Thermodynamics of cell penetrating peptides on lipid membranes: sequence and membrane acidity regulate surface binding. Phys Chem Chem Phys 22:23399–23410. https://doi.org/10.1039/d0cp02770g

Rathnayake PVGM, Gunathunge BGCM, Wimalasiri PN et al (2017) Trends in the binding of cell penetrating peptides to siRNA: a molecular docking study. J Biophys 2017:1–12. https://doi.org/10.1155/2017/1059216

Rhee M, Davis P (2006) Mechanism of uptake of C105Y, a novel cell-penetrating peptide. J Biol Chem. https://doi.org/10.1074/jbc.M509813200

Rojas M, Donahue JP, Tan Z, Lin Y-Z (1998) Genetic engineering of proteins with cell membrane permeability. Nat Biotechnol. https://doi.org/10.1038/nbt0898-773

Ruseska I, Zimmer A (2020) Internalization mechanisms of cell-penetrating peptides. Beilstein J Nanotechnol 11:101–123. https://doi.org/10.3762/bjnano.11.10

Ruzza P, Biondi B, Marchiani A et al (2010) Cell-penetrating peptides: a comparative study on lipid affinity and cargo delivery properties. Pharmaceuticals 3:1045–1062. https://doi.org/10.3390/ph3041045

Rydberg HA, Matson M, Åmand HL et al (2012) Effects of tryptophan content and backbone spacing on the uptake efficiency of cell-penetrating peptides. Biochemistry 51:5531–5539. https://doi.org/10.1021/bi300454k

Sagan S (2013) Cell-penetrating peptides: 20 years later, where do we stand? FEBS Lett 587:1693

Said Hassane F, Saleh AF, Abes R et al (2010) Cell penetrating peptides: overview and applications to the delivery of oligonucleotides. Cell Mol Life Sci 67:715–726. https://doi.org/10.1007/s00018-009-0186-0

Schmidt N, Mishra A, Lai GH, Wong GCL (2010) Arginine-rich cell-penetrating peptides. FEBS Lett 584:1806–1813. https://doi.org/10.1016/j.febslet.2009.11.046

Shen Y, Maupetit J, Derreumaux P, Tufféry P (2014) Improved PEP-FOLD approach for peptide and miniprotein structure prediction. J Chem Theory Comput 10:4745–4758. https://doi.org/10.1021/ct500592m

Silva S, Almeida AJ, Vale N (2019) Combination of cell-penetrating peptides with nanoparticles for therapeutic application: a review. Biomolecules 9:1–24. https://doi.org/10.3390/biom9010022

Trabulo S, Cardoso AL, Mano M, de Lima MCP (2010) Cell-penetrating peptides-mechanisms of cellular uptake and generation of delivery systems. Pharmaceuticals 3:961–993. https://doi.org/10.3390/ph3040961

Van Der Spoel D, Lindahl E, Hess B et al (2005) GROMACS: fast, flexible, and free. J Comput Chem 26:1701–1718. https://doi.org/10.1002/jcc.20291

Wassenaar TA, Ingólfsson HI, Böckmann RA et al (2015) Computational lipidomics with insane: a versatile tool for generating custom membranes for molecular simulations. J Chem Theory Comput 11:2144–2155. https://doi.org/10.1021/acs.jctc.5b00209

Wrighton CJ, Hofer-Warbinek R, Moll T et al (1996) Inhibition of endothelial cell activation by adenovirus-mediated expression of I kappa B alpha, an inhibitor of the transcription factor NF-kappa B. J Exp Med 183:1013–1022. https://doi.org/10.1084/jem.183.3.1013

Yesylevskyy S, Marrink SJ, Mark AE (2009) Alternative mechanisms for the interaction of the cell-penetrating peptides penetratin and the TAT peptide with lipid bilayers. Biophys J 97:40–49. https://doi.org/10.1016/j.bpj.2009.03.059

Zhang L, Torgerson TR, Liu XY et al (1998) Preparation of functionally active cell-permeable peptides by single-step ligation of two peptide modules. Proc Natl Acad Sci U S A. https://doi.org/10.1073/pnas.95.16.9184